

Thermal expansion and the glass transition

Peter Lunkenheimer^{1✉}, Alois Loidl¹, Birte Riechers^{2,3}, Alessio Zaccone^{4,5,6} and Konrad Samwer⁷

¹ Experimental Physics V, Center for Electronic Correlations and Magnetism, University of Augsburg, 86135 Augsburg, Germany

² Bundesanstalt für Materialforschung und -prüfung, Unter den Eichen 87, 12205 Berlin, Germany

³ Glass and Time, Department of Science and Environment, Roskilde University, DK-4000 Roskilde, Denmark

⁴ Department of Physics "A. Pontremoli", University of Milan, Via Celoria 16, 20133 Milan, Italy

⁵ Department of Chemical Engineering and Biotechnology, University of Cambridge, Cambridge CB3 0AS, U.K.

⁶ Cavendish Laboratory, University of Cambridge, Cambridge, CB3 0HE, U.K.

⁷ 1. Physikalisches Institut, University of Goettingen, Germany

Melting is well understood in terms of the Lindemann criterion, essentially stating that crystalline materials melt when the thermal vibrations of their atoms become such vigorous that they shake themselves free of the binding forces. However, how about another common type of solids: glasses, where the nature of the solid-liquid crossover is highly controversial? The Lindemann criterion implies that the thermal expansion coefficients α of crystals are inversely proportional to their melting temperatures. Here we find that, unexpectedly, α of glasses decreases much stronger with increasing glass-transition temperature T_g marking the liquid-solid crossover in this material class. However, scaling α by the fragility m , a measure of particle cooperativity, restores the proportionality, i.e., $\alpha/m \propto 1/T_g$. Obviously, for a glass to become liquid, it is not sufficient to simply overcome the interparticle binding energies. Instead, more energy has to be invested to break up the typical cooperative particle network which is considered a hallmark feature of glassy materials. Surprisingly, α of the liquid phase reveals similar anomalous behaviour and is universally enhanced by a constant factor of ~ 3 . The found universalities allow estimating glass-transition temperatures from thermal expansion and vice versa.

Many materials in technology and nature are glasses, disordered materials that are solid but lack the periodicity of the crystalline lattice^{1,2}. This not only includes the common silica-based transparent materials used for windows, glass fibres, etc., but also many polymers and bio-derived materials, various solid-state electrolytes, supercooled molecular liquids and even amorphous metals. This state of matter is usually prepared by cooling a liquid sufficiently fast to avoid crystallization^{1,2,3}. Below the melting temperature T_m , then a so-called supercooled liquid is formed first, before the material becomes a glass below the glass-transition temperature $T_g < T_m$. The latter marks the boundary between liquid and solid which usually is defined at a viscosity value of 10^{12} Pas. However, in contrast to crystallization, the solidification at T_g occurs smoothly, i.e. without a discontinuous jump of the viscosity. Below T_g , most physical quantities of a glass former exhibit a crossover to weaker temperature dependence, i.e. a jump in their derivatives, at first glance reminding of a second-order phase transition. This is also the case for the volume (cf. Fig. 1a), respectively the thermal expansion, treated in the present work.

Although mankind is using supercooling for the preparation of glasses since millennia, there is no consensus on the true nature of the glass transition^{1,2,3,4,5}. The temperature of the mentioned crossover depends on the cooling rate, clearly excluding a canonical phase transition. Instead, it is commonly assumed that the liquid falls out of thermodynamic equilibrium at the glass transition, which happens just at T_g for a typical cooling rate of 10 K/min. Nevertheless, various

competing theoretical approaches assume that an underlying, "hidden" phase transition at a temperature above or below T_g may in fact govern the crossover between liquid and glass^{2,4,6,7}. Alternatively, it simply could be a purely kinetic phenomenon^{4,8,9}.

In contrast, the transition between the liquid and solid states via crystallization and melting is much better understood¹⁰, in particular in terms of the basic ideas behind the Lindemann criterion^{11,12}. The latter predicts that melting occurs when the root mean-square (rms) displacement of particles due to thermal vibrations exceeds a certain percentage of the interparticle spacing¹², often reported to be roughly of the order of 10 % (refs. ^{13,14,15}). It is nowadays well established that these vibrations take place within potential wells whose asymmetry gives rise to thermal expansion. The higher the melting temperature, the deeper the well, and, hence, the steeper the slope of its attractive part should be (cf. Fig. 1b). As this slope s is related to the thermal-expansion coefficient α_c of a crystalline material, one can expect less expansion for materials with higher T_m . Making the reasonable approximations that $T_m \propto U_0$ (with U_0 the depth of the well) and that $1/\alpha_c \propto s \propto U_0$ (ref. ¹⁶; see Supplementary Note 1 for a more detailed discussion), one arrives at:

$$\alpha_c T_m = \text{const.} \quad (1)$$

Here α_c is defined as the relative volume change at constant pressure p , namely $\alpha_c = 1/V (\partial V/\partial T)_p$. Indeed, such a relation

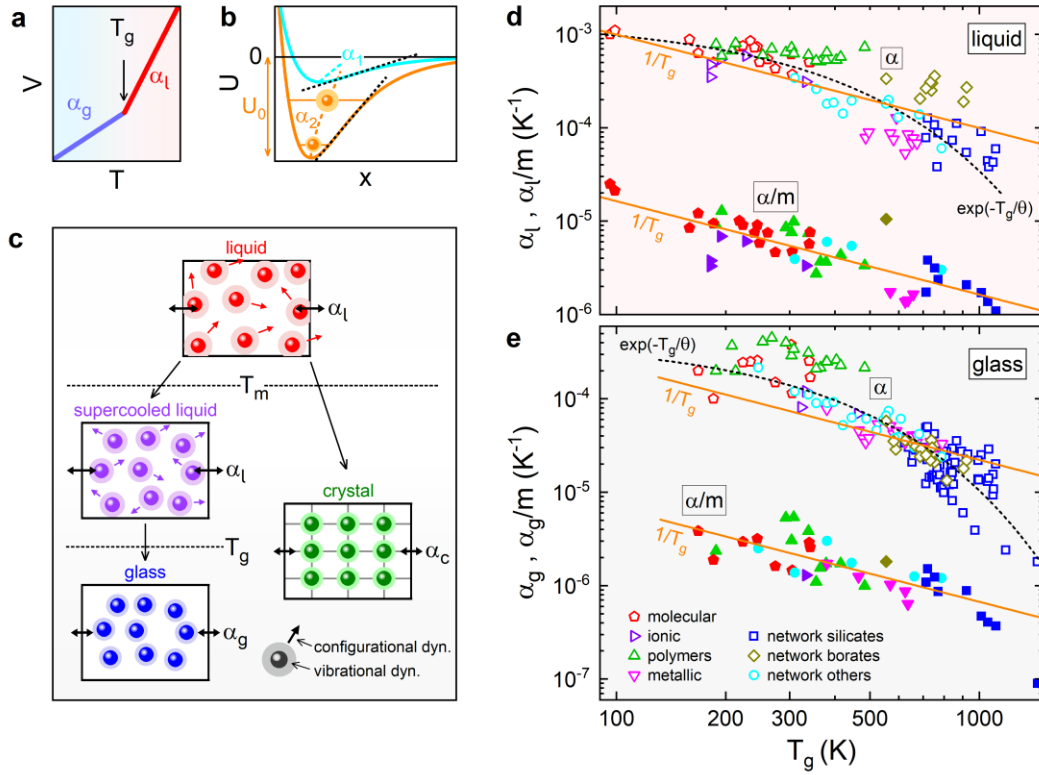


Fig. 1 Contributions to the thermal expansion and its correlations with the glass-transition temperature. **a**, Schematic plot of the temperature variation of the volume around the glass transition. **b**, Schematic plot of the asymmetric pair potential giving rise to thermal expansion in a solid. Two potentials for two different binding energies (depths of minima) are shown. The dotted black lines show the slopes at the attractive parts of the potentials which are smaller for lower binding energy. The dashed lines indicate the average location of the particle which shifts to the right (larger interparticle distance) for higher temperature, leading to thermal expansion. For the deeper potential, the particle position is shown for two temperatures. **c**, Schematic presentation of the different contributions to the thermal expansion of liquids, glasses and crystals: the vibrational dynamics is indicated by the shaded areas around the spheres, representing the atoms or molecules of the material. The additional configurational dynamics in the liquid phases is indicated by single-headed arrows. The double-headed arrows illustrate the resulting thermal expansion. **d,e**, Double-logarithmic plot of the experimentally-determined thermal volume-expansion coefficients α_g in the glass phase (**d**) and of α_l in the liquid phase (**e**) versus the glass-transition temperature T_g for a large variety of glass formers belonging to different material classes (see Supplementary Table 1 for detailed information on all materials and values and the corresponding references). In addition to the bare expansion coefficients (open symbols), the figure also provides the α values divided by the fragility parameter m (filled symbols) being a measure of cooperative dynamics. The solid lines show linear fits with slope -1, based on all data points for each phase, except for α_l of the borates. The dashed lines represent fits with $\alpha \propto \exp(-T_g/\theta)$ with the same $\theta \approx 270$ K for both data sets. Note that the ordinates of (**d**) and (**e**) were adjusted to achieve the same decades/cm ratio.

was suggested to be directly related to the Lindemann criterion^{14,17} (see also Supplementary Note 1).

In crystalline solids, the ordered structure melts at the melting temperature and in glasses the rigid disordered structure dissolves above the glass-transition temperature. Thus, it seems natural that these two phenomena have a common basis, specifically having in mind that for many glasses the relation $T_g \approx 2/3 T_m$ holds^{18,19,20,21,22} (but also exceptions were reported²³). In light of a possible Lindemann-like criterion for the glass-liquid transition considered, e.g., in refs. 4,21,22,24,25,26,27,28, in analogy to crystals one thus may expect the relation

$$\alpha_g T_g = \text{const.} \quad (2)$$

In general, the thermal expansion is of fundamental importance, defining universal quantities such as the Grüneisen parameter or the Prigogine-Defay ratio^{1,12,29}. It also reflects the occurrence of different dynamic processes in glasses.³⁰ The change of slope of $V(T)$ at T_g (Fig. 1a) is one of the most paradigmatic characteristics of the glass transition^{18,31,32}. The thermal-expansion coefficient in liquids, α_l , is by about a factor of 1.5 - 4 higher than in solids^{32,33,34,35}. It is well established that α_l contains two contributions: a vibrational one, also present in the solid state, and an additional configurational one, being caused by the

translational motions of the particles that also give rise to the viscous flow defining a liquid^{22,33,34,36} (see schematic representation in Fig. 1c). The vibrational contribution arises from the anharmonic interparticle potential and dominates the thermal expansions of crystals and glasses, which mostly are of similar magnitude.

Interestingly, Stillinger and co-workers suggested a Lindemann-like *freezing* criterion for liquids^{37,38,39}: Based on molecular-dynamics simulations, they found that melts freeze if the rms particle displacement falls below about one-half of the interparticle spacing. In analogy to equations (1) and (2), related to the Lindemann *melting* criterion, one thus could naively expect

$$\alpha_l T_g = \text{const.} \quad (3)$$

with α_l the expansion coefficient of the liquid. However, α_l is believed to be governed by additional configurational motions instead of the vibrations exclusively considered in the Lindemann scenario. Therefore, deviations from such a correlation, if present at all, may be expected. Nevertheless, in ref. ⁴⁰ such a relation was predicted, based on theoretical considerations. Moreover, within the framework of the recently developed Krausser-Samwer-Zaccone (KSZ) model⁴¹, equation (3) should also be approximately valid. In this model, a steepness parameter λ determines the repulsive part of the inter-particle potential and is a proxy for the chemistry-dependent bonding. If $\alpha_l T_g$ is independent of λ , *i.e.* of chemistry, KSZ predict an approximately linear relation between the fragility index m (refs. ^{42,43}) and λ . Indeed, this prediction was recently found to be fulfilled for a large variety of glass formers⁴⁴, in accord with equation (3).

In literature there are some reports on, partly contradicting, correlations of T_g with the thermal expansion or with $\Delta\alpha$, the jump of α at T_g , namely: $\Delta\alpha T_g = \text{const.}$ ^{45,46}, $\Delta\alpha T_g \propto T_g$ (ref. ⁴⁷), $\alpha_g T_g^2 = \text{const.}$ ²⁰, and $\alpha_l T_g = \text{const.}$ ^{40,45} (equation (3)). However, they all were found for specific classes of glass-formers only and the overall data base was limited. In contrast, in the present work, using data on more than 200 materials from literature (see Supplementary Table 1), we check for such correlations across very different classes of glass formers.

If equations (2), (3) or alternative universal relations hold, α measured in a glass or liquid would allow to predict glass-transition temperatures, without any knowledge of microscopic pair-potential parameters. At the same time, one could gain insight into the universality of configurational contributions to the thermal expansion at $T > T_g$ and concerning the relevance of a Lindemann-like mechanism for the glass transition. In any case, the explanation of a possible universal relationship of α and T_g would represent a severe benchmark for any model of the glass transition.

Experimental data and analysis

The values of α_g , α_l and T_g used in the present work are listed in Supplementary Table 1 and details on their selection and reliability are provided in the Supplementary Notes 2 and 3. The included materials can be classified as molecular glass

formers (alcohols, van-der-Waals bonded and other systems), polymers, ionic glass formers (including ionic liquids and melts), metallic systems (so-called bulk metallic glasses and others), and network glass formers (including silicates, borates, phosphates, chalcogenides and halogenides). Their interparticle bond types vary from covalent, hydrogen, ionic, metallic to van-der-Waals bonds. Their glass-transition temperatures cover about one decade and their thermal-expansion coefficients vary by approximately 2.5 and 1.5 decades in the glass and liquid phases, respectively. In general, the available data basis is broader for the glass state than for the liquid phase.

The open symbols in Figs. 1d and e show the complete $\alpha(T_g)$ data sets for the liquid and glass states, respectively, using a double-logarithmic representation. The first conclusion from these figures is a clear correlation of the thermal expansion with the glass-transition temperature, namely a decrease of α_g and α_l with increasing T_g . Notably, this correlation holds across very diverse material classes (indicated by different symbols in the figures) with different bond types and drastically varying glass-transition temperatures. The scatter of the data certainly partly signals the fact that α was often measured employing very different techniques applied by various experimental groups during the last century. It probably also arises from variations in the width and separation from T_g of the temperature regime where the thermal expansion was determined (see also Supplementary Notes 2 and 3).

As discussed above, in principle a decrease of α with increasing T_g , as demonstrated in Figs. 1d and e, is expected if a Lindemann-like scenario would apply for the glass-liquid transition, too. However, when assuming the validity of equations (2) and (3), such double-logarithmic plots of α versus T_g (open symbols) should lead to approximately linear behaviour with slope -1. Instead, both data sets depend much stronger on T_g as becomes obvious from a comparison with the upper solid lines, indicating slope -1, *i.e.* $\alpha \propto 1/T_g$. At best, only part of the liquid data, especially at $T_g < 400$ K, are roughly consistent with equation (3). This rationalizes the reported correlation of λ with the fragility index m (ref. ⁴⁴) within the framework of the KSZ model⁴¹. We find that an exponential T_g -dependent variation, $\alpha_i = \alpha_{0,i} \exp(-T_g/\theta_i)$ (with $i = g$ or l for glass or liquid, respectively), as indicated by the dashed lines in Figs. 1d and e, provides a much better formal description of the experimental data than $\alpha_i \propto 1/T_g$ suggested by equations (2) and (3). Indeed, both data sets can be quite well linearized within a semi-logarithmic representation, plotting the logarithm of α_i versus T_g (Supplementary Fig. 1). The only exception are the values for the borates in the liquid state, whose thermal expansion seems to represent a special case. Indeed, exceptional thermal-expansion properties of the borate glasses were identified earlier^{19,48,49}, and are believed to be due to their specific network structure.

The very similar α - T_g correlations for the liquid and glass state are astonishing, having in mind that the thermal expansion in the supercooled liquid includes vibrational as well as configurational contributions, while in the glass it should be dominated by vibrational contributions only.

Moreover, we find an approximately identical exponential factor $\theta = \theta_g \approx 270$ K, for both glasses and liquids. This implies a fixed ratio $\alpha_l/\alpha_g = \alpha_{0,l}/\alpha_{0,g}$. Using $\alpha_{0,l} \approx 1.4 \times 10^{-3} \text{ K}^{-1}$ and $\alpha_{0,g} \approx 4.3 \times 10^{-4} \text{ K}^{-1}$, obtained from the fits, this ratio is about three, which should be universally valid for all glass formers. To check this prediction, Fig. 2 shows α_l/α_g versus T_g for those materials where both expansion coefficients are available. Indeed, this ratio is close to three for a large variety of glass-formers belonging to different material classes. Only the borate glasses reveal much larger ratios, in accord with their known anomalous expansion behaviour^{19,48,49}.

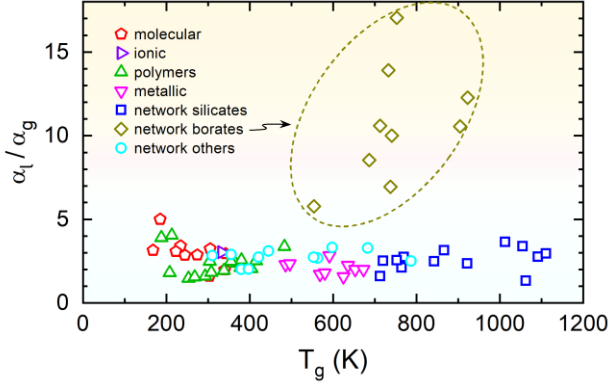


Fig. 2 | Ratio of the thermal expansion coefficients measured in the liquid and glass phases. Leaving the borate glasses aside, this ratio is of order three for all systems and independent of the glass-transition temperature.

Discussion and Concluding remarks

We have shown that the thermal-expansion data of about 200 glass formers reveal a clear correlation with the glass-transition temperature, which holds across vastly different material classes. However, the data are clearly inconsistent with $\alpha T_g = \text{const.}$, expected when assuming a Lindemann-like scenario for the glass transition. This expectation is neither met for the glass, nor for the liquid phase, where it was theoretically predicted^{40,41,44}. Instead, we find a much stronger decrease of α with T_g for both states. This only becomes obvious when considering data covering a broad range of glass-transition temperatures and thermal-expansion coefficients.

The invalidity of equation (2) implies that at least one of the intuitive proportionalities $T_g \propto U_0$ and $1/\alpha_g \propto U_0$ (analogous to the crystal case; cf. introduction section and Supplementary Note 1) must be invalid for glasses. A clue is given when considering that U_0 , the depth of the pair potential, essentially corresponds to the interparticle binding strength. As materials with very weak (van-der-Waals) and strong (covalent) bonds are included here, it should vary by about 2 - 3 decades. This is in accord with the observed variation of α_g (Fig. 1e), i.e. consistent with $1/\alpha_g \propto U_0$. In contrast, T_g varies by 1.2 decades only and, thus, $T_g \propto U_0$ should be invalid. Therefore, we conclude that the transition temperature from glass to liquid depends much weaker on the microscopic quantity U_0 than for the crystal-liquid transition where $T_m \propto U_0$. This marked difference seems to somehow

reflect the fact that the glass transition qualitatively differs from crystal melting. This can be rationalized as follows:

Notably, the systems with small T_g and high α , lying in the upper left part of Fig. 1e (e.g., the polymers and molecular materials), generally exhibit higher fragility index m than those with high T_g and small α like the metallic or network systems⁵⁰ (cf. Supplementary Table 1). m is a quantitative measure of the deviation of a material's viscosity η from the Arrhenius temperature dependence, $\eta \propto \exp[E/(k_B T)]$, expected when assuming canonical thermally-activated particle dynamics with a well-defined energy barrier E (refs. ^{42,43}). Such deviations are a hallmark feature of glass-forming liquids and strongly material dependent, being most pronounced, e.g., in many polymers and molecular liquids^{1,4,43}. They are often ascribed to an increase of the effective energy barrier with decreasing temperature, caused by the cooperative motion of ever larger numbers of molecules upon cooling a liquid towards its glass transition^{2,3,51}. Within this framework, higher m values (characterizing so-called "fragile" glass formers^{1,4,43}) mean that this increase is stronger than for small m values ("strong" glass formers).

The stronger T_g dependence of α_g compared to equation (2), observed in the present work, then could be due to this effective energy-barrier enhancement: The glass temperatures of the more fragile materials in the upper left part of Fig. 1e are larger than expected from their pair-potential depth alone, because, in order to liquify these glasses, more energy has to be invested to break up their cooperative particle network. Within this scenario, $T_g \propto m U_0$ instead of $T_g \propto U_0$ may be tentatively assumed. In contrast, the relation $\alpha_g \propto 1/U_0$ should be unaffected by cooperativity as thermal expansion is governed by the local pair potential only (Fig. 1b). Therefore, the proportionality $\alpha_g \propto 1/T_g$ should be invalid, in accord with experimental observation (Fig. 1e), and, instead, the quantity α_g/m should be proportional to $1/T_g$. This expectation indeed is well fulfilled as demonstrated by the filled symbols in Fig. 1e, showing α_g/m vs. T_g for those systems where m is known (cf. Supplementary Table 1). Notably, a corresponding cooperativity correction also is able to linearize the thermal expansion coefficients of the liquid state (filled symbols in Fig. 1d), i.e., we find $\alpha_l/m \propto 1/T_g$. Thus equations (2) and (3) should be replaced by:

$$\alpha_i/m T_g = \text{const.} \quad (i = g, l) \quad (4)$$

Finally, it is remarkable that α_l and α_g (or α_l/m and α_g/m) exhibit the same dependence on glass temperature and are related by a universal factor of about three, characterizing the increase of the thermal expansion when crossing the glass transition upon heating. A factor of 2 - 4 was occasionally quoted in literature^{33,34} and here we document a factor close to 3 which is valid for the complete universe of glass-forming materials, leaving the borates aside. As discussed above, it is reasonable that the vibrational contributions to the thermal expansion are essentially the same in the glass and liquid states (cf. Fig. 1c), ascribing the observed higher α_l to additional configurational contributions arising above T_g (refs. ^{33,34}). Then $\alpha_l/\alpha_g \approx 3$ implies that the configurational part is

universally two times higher than the vibrational one, which seems surprising when considering their different physical origins. It is reasonable that the thermal expansion is related to the maximum possible displacement of a particle during the corresponding motion (either vibrational and/or configurational). If one expands the 3rd derivative of the pair potential versus distance (the thermal expansion coefficient) from one to three dimensions, assuming still the same local process, and adds the configurational – many body – motions, one can rationalize the detected factor of three. Thus, we conclude that the enhancement of α above T_g is essentially a dimensionality effect. Locally we propose here the crossover from a two-body interaction (vibrations on the ps timescale) to an additional many-body process (configurational changes on a much longer time scale).

The found universal correlation of α_g and T_g , involving the degree of cooperativity of particle motion in different material classes, quantified by fragility m , obviously is a typical, so far unnoticed, property of glasses. It markedly differs from the much simpler behaviour of crystalline systems which can be explained in terms of the Lindemann criterion. This and the unexpected universal factor relating α in the glass to that in the liquid put severe constraints on existing and future models of the glass transition. Finally, the present results have predictive power for engineering glassy materials by design: one will be able to predict T_g in a bottom-up way based on interatomic/intermolecular parameters and to deduce it from a simple thermal expansion measurement; conversely, a simple T_g measurement will yield a wealth of information about atomic-scale composition and thermal properties.

Data availability

The data that support the findings of this study are available in Supplementary Table 1.

Acknowledgements

We thank Gyan Johari, Frank Stillinger and Dieter Vollhardt for stimulating discussions. K.S. acknowledges constant support over many years by the DFG Sa/337 via the Leibniz Program and Caltech, Pasadena, CA via the visiting associate program. B.R. is grateful for support from the VILLUM Foundation's Matter Grant (No. 16515). A.Z. gratefully acknowledges financial support from US Army Research Office, Contract No. W911NF-19-2-0055.

Author Contributions

K.S. initiated this work. P.L. and B.R. collected the experimental data. P.L. analyzed the data and prepared the figures. A.L., P.L., K.S., and A.Z. wrote the manuscript. All authors discussed the results and commented on the manuscript.

Competing interests

The authors declare no competing interests.

Additional information

Supplementary information The online version contains supplementary material available at...

Correspondence and requests for materials should be addressed to Peter Lunkenheimer.

References

- Angell, C. A. Formation of glasses from liquids and biopolymers. *Science* **267**, 1924-1935 (1995).
- Debenedetti, P. G. & Stillinger, F. H. Supercooled liquids and the glass transition. *Nature* **410**, 259-267 (2001).
- Kivelson, S. A. & Tarjus, G. In search of a theory of supercooled liquids. *Nature Mater.* **7**, 831-833 (2008).
- Ediger, M. D., Angell, C. A. & Nagel, S. R. Supercooled liquids and glasses. *J. Phys. Chem.* **100**, 13200-13212 (1996).
- Dyre, J. C. Colloquium: The glass transition and elastic models of glass-forming liquids. *Rev. Mod. Phys.* **78**, 953-972 (2006).
- Kirkpatrick, T. R. & Wolynes, P. G. Stable and metastable states in mean-field Potts and structural glasses. *Phys. Rev. B* **36**, 8552-8564 (1987).
- Albert, S., Bauer, Th., Michl, M., Biroli, G., Bouchaud, J.-P., Loidl, A., Lunkenheimer, P., Tourbot, R., Wiertel-Gasquet, C. & Ladieu, F. Fifth-order susceptibility unveils growth of thermodynamic amorphous order in glass-formers. *Science* **352**, 1308-1311 (2016).
- Angell, C. A. & Rao, K. J. Configurational excitations in condensed matter, and the "bond lattice" model for the liquid-glass transition. *J. Chem. Phys.* **57**, 470-481 (1972).
- Chandler, D. & Garrahan, J. P. Dynamics on the way to forming glass: Bubbles in space-time. *Annu. Rev. Phys. Chem.* **61**, 191-217 (2010).
- Cahn, R. W. Melting from within. *Nature* **513**, 582-583 (2001).
- Lindemann, F. A. The calculation of molecular vibration frequencies. *Phys. Z.* **11**, 609-612 (1910).
- Gilvary, J. J. The Lindemann and Grüneisen Laws. *Phys. Rev.* **102**, 308-316 (1956).
- Stillinger, F. H. & Weber, T. A. Lindemann melting criterion and the Gaussian core model. *Phys. Rev. B* **22**, 3790-3794 (1980).
- Granato, A. V., Joncich, D. M. & Khonik, V. A. Melting, thermal expansion, and the Lindemann rule for elemental substances. *Appl. Phys. Lett.* **97**, 171911 (2010).
- Lawson, A. C. Physics of the Lindemann melting rule. *Phil. Mag.* **89**, 1757-1770 (2009).
- MacDonald, D. K. C. & Roy, S. K. Vibrational anharmonicity and lattice thermal properties, II, *Phys. Rev.* **97**, 673-676 (1955).
- Shi, B., Yang, S., Liu, S. & Jin, P. Lindemann-like rule between average thermal expansion coefficient and glass transition temperature for metallic glasses. *J. Non-Cryst. Solids* **503-504**, 194-196 (2019).
- Sakka, S. & MacKenzie, J. D. Relation between apparent glass transition temperature and liquids temperature for inorganic glasses. *J. Non-Cryst. Solids* **6**, 145-162 (1971).
- Scholze, H. *Glas: Natur, Struktur und Eigenschaften* (Springer, Berlin, 1988).
- Van Uitert, L. G. Relations between melting point, glass transition temperature, and thermal expansion for inorganic crystals and glasses. *J. Appl. Phys.* **50**, 8052-8061 (1979).
- Malinovsky, V. K. & Novikov, V. N. The nature of the glass transition and the excess low energy density of vibrational states in glasses. *J. Phys.: Condens. Matter* **4**, L139-L143 (1992).
- Angell, C. A., Ngai, K. L., McKenna, G. B., McMillan, P. F. & Martin, S. W. Relaxation in glass forming liquids and amorphous solids. *J. Appl. Phys.* **88**, 3113-3157 (2000).

- ²³ Lu, Z. & Lia, J. Correlation between average melting temperature and glass transition temperature in metallic glasses. *Appl. Phys. Lett.* **94**, 061913 (2009).
- ²⁴ Xia, X. Y. & Wolynes, P. G. Fragilities of liquids predicted from the random first order transition theory of glasses. *Proc. Natl. Acad. Sci.* **97**, 2990-2994 (2000).
- ²⁵ Larini, L., Ottochian, A., De Michele, C. & Leporini, D. Universal scaling between structural relaxation and vibrational dynamics in glass-forming liquids and polymers. *Nature Phys.* **4**, 42-45 (2007).
- ²⁶ Chakravarty, Ch., Debenedetti, P. G. & Stillinger, F. H. Lindemann measures for the solid-liquid phase transition. *J. Chem. Phys.* **126**, 204508 (2007).
- ²⁷ Zaccone, A. & Terentjev, E. Disorder-assisted Melting and the glass transition in amorphous solids. *Phys. Rev. Lett.* **110**, 178002 (2013).
- ²⁸ Sanditov, D. S. A criterion for the glass-liquid transition. *J. Non-Cryst. Solids* **385**, 148-152 (2014).
- ²⁹ Schmelzer, J. W. P. & Gutzow, I. The Prigogine-Defay ratio revisited. *J. Chem. Phys.* **125**, 184511 (2006).
- ³⁰ Simha, R. Transitions, relaxations, and thermodynamics in the glassy state. *Polym. Eng. Sci.* **20**, 82-86 (1980).
- ³¹ Zarzycki, J. *Glasses and the Vitreous State* (Cambridge University Press, 1991).
- ³² Kauzmann, W. The nature of the glassy state and the behavior of liquids at low temperatures. *Chem. Rev.* **43**, 219-256 (1948).
- ³³ Stillinger, F. H. & Debenedetti, P. G. Distinguishing vibrational and structural equilibration contributions to thermal expansion. *J. Phys. Chem. B* **103**, 4052-4059 (1999).
- ³⁴ Johari, G. P. Determining vibrational heat capacity and thermal expansivity and their change at glass-liquid transition. *J. Chem. Phys.* **126**, 114901 (2007).
- ³⁵ Davies, R. O. & Jones, G. O. Thermodynamic and kinetic properties of glasses. *Adv. Phys.* **2**, 370-410 (1953).
- ³⁶ Potuzak, M., Mauro, J. C., Kiczenski, T. J., Ellison, A. J. & Allan, D. C. Resolving the vibrational and configurational contributions to thermal expansion in isobaric glass-forming systems. *J. Chem. Phys.* **133**, 091102 (2010).
- ³⁷ Stillinger, F. H. A topographic view of supercooled liquids and glass formation. *Science* **265**, 1935-1939 (1995).
- ³⁸ Stillinger, F. H. & Weber, T. A. Computer simulation of local order in condensed phases of silicon. *Phys. Rev. B* **31**, 5262-5271 (1985).
- ³⁹ Lavolette, R. A. & Stillinger, F. H. Multidimensional geometric aspects of the solid liquid transition in simple substances. *J. Chem. Phys.* **83**, 4079-4085 (1985).
- ⁴⁰ Wool, R. P. Twinkling fractal theory of the glass transition. *J. Polym. Sci., Part B: Polym. Phys.* **46**, 2765-2778 (2008).
- ⁴¹ Krausser, J., Samwer, K. H. & Zaccone, A. Interatomic repulsion softness directly controls the fragility of supercooled metallic melts. *Proc. Natl. Acad. Sci. U.S.A.* **112**, 13762-13767 (2015).
- ⁴² Plazek, D. J. & Ngai, K. L. Correlation of polymer segmental chain dynamics with temperature-dependent time-scale shifts. *Macromolecules* **24**, 1222-1224 (1991).
- ⁴³ Böhmer, R. & Angell, C. A. Correlations of the nonexponentiality and state dependence of mechanical relaxations with bond connectivity in Ge-As-Se supercooled liquids. *Phys. Rev. B* **45**, 10091-10094 (1992).
- ⁴⁴ Lunkenheimer, P., Humann, F., Loidl, A. & Samwer, K. Universal correlations between the fragility and the interparticle repulsion of glass-forming liquids. *J. Chem. Phys.* **153**, 124507 (2020).
- ⁴⁵ Simha, R. & Boyer, R. F. On a general relation involving the glass temperature and coefficients of expansion of polymers. *J. Chem. Phys.* **37**, 1003-1007 (1962).
- ⁴⁶ Boyer, R. F. & Simha, R. Relation between expansion coefficients and glass temperature: A reply. *Polymer Letters* **11**, 33-44 (1973).
- ⁴⁷ Sharma, S. C., Mandelkern, L. & Stehling, F. C. Relation between expansion coefficients and glass temperature. *Polymer Letters* **10**, 345-356 (1972).
- ⁴⁸ Shelby, J. E. Thermal expansion of alkali borate glasses. *J. Amer. Ceram. Soc.* **66**, 225-227 (1983).
- ⁴⁹ Shelby, J. E. Properties and structure of B₂O₃-GeO₂ glasses. *J. Appl. Phys.* **45**, 5272-5277 (1974).
- ⁵⁰ Böhmer, R., Ngai, K. L., Angell, C. A. & Plazek, D. J. Nonexponential relaxations in strong and fragile glass formers, *J. Chem. Phys.* **99**, 4201-4209 (1993).
- ⁵¹ Bauer, Th., Lunkenheimer, P. & Loidl, A. *Cooperativity and the freezing of molecular motion at the glass transition*, *Phys. Rev. Lett.* **111**, 225702 (2013).

Supplementary Information

for

Thermal expansion and the glass transition

Peter Lunkenheimer¹, Alois Loidl¹, Birte Riechers^{2,3}, Alessio Zaccone^{4,5,6} and Konrad Samwer⁷

¹ Experimental Physics V, Center for Electronic Correlations and Magnetism, University of Augsburg, 86135 Augsburg, Germany

² Bundesanstalt für Materialforschung und -prüfung, 12205 Berlin, Germany

³ Glass and Time, Department of Science and Environment, Roskilde University, DK-4000 Roskilde, Denmark

⁴ Department of Physics "A. Pontremoli", University of Milan, Via Celoria 16, 20133 Milan, Italy

⁵ Department of Chemical Engineering and Biotechnology, University of Cambridge, Cambridge CB3 0AS, U.K.

⁶ Cavendish Laboratory, University of Cambridge, Cambridge, CB3 0HE, U.K.

⁷ 1. Physikalisches Institut, University of Goettingen, Germany

Contents:

Supplementary Note 1

Supplementary Note 2

Supplementary Note 3

Supplementary Figure 1 (with discussion)

Supplementary Table 1

Supplementary Table 2

References

Supplementary Note 1: The Lindemann criterion and alternative melting rules for crystals

The first melting rule that gained considerable attention is generally assigned to Lindemann.¹ More than 100 years ago, he calculated the phonon frequencies of monoatomic materials from the melting temperature T_m utilizing Einstein frequencies and assuming that at the melting temperature the atoms with a given vibrational amplitude touch each other. This Lindemann melting criterion was brought into his modern form mainly by work of Gilvarry² reformulating the melting criterion in terms of root mean-square (rms) phonon displacements and utilizing the Debye model in calculating the phonon eigenfrequencies. His main conclusion was that monoatomic crystals melt when their mean-square displacements reach a critical value of their vibrational amplitude which is of the order of 7 – 8 % of the next-nearest neighbor distance. Nowadays, the Lindemann criterion of melting usually implies a ratio of rms displacements of particles to the lattice spacing of order 0.05 – 0.16 (e.g., ref. 3).

The Lindemann melting criterion can be derived using phonon excitation in a strictly harmonic potential, while in any realistic melting process, anharmonic contributions to the pair potential, giving rise to thermal expansion, will play an essential role. In addition, thermal expansivity certainly can be much easier measured than rms displacements and early on there were attempts to derive melting rules including anharmonic lattice effects. The very first remarkable attempt was provided by Grüneisen⁴. Assuming a realistic lattice potential including attractive and repulsive interaction forces, he calculated a number of important thermodynamic quantities via a rather complete and probably the first equation of state for crystalline solids, where the dimensionless parameter γ enters, which was later named Grüneisen-parameter. Amongst many other quantities, he calculated the volume expansion from 0 K to the melting temperature and derived the equation $(V_m - V_0)/V_0 = \text{const.}$, where V_m and V_0 denote the volume at the melting temperature and at 0 K, respectively. For monoatomic elements, Grüneisen found this constant characterizing the relative volume expansion from 0 K to the melting point to be of order ~ 0.08 .⁴ From this relation one can immediately derive the condition $\alpha_c T_m = \text{const.}$, with T_m being the melting temperature and α_c the coefficient of thermal expansion in the crystalline state, assumed to be constant up to the melting temperature. The relation of Grüneisen's treatment and the Lindemann melting criterion were discussed in detail by Dugdale and MacDonald⁵, by MacDonald and Roy,⁶ and by Gilvarry.² These authors also documented that the derivation of Grüneisen is valid for different types of anharmonic potentials and that, in first respect, the Grüneisen-parameter describes the characteristic lattice anharmonicity. Remarkably, Grüneisen recalculated the mean amplitude of a single atom at the melting temperature and derived a ratio of 0.085 compared to the interatomic separation.

Taking the above given relation, $\alpha_c T_m = \text{const.}$, serious, implies that the involved quantities, the melting temperature as well as the coefficient of thermal expansion, both depend on the strength of the interatomic pair potential. One can expect that T_m is proportional to the depth of the pair potential, U_0 . Considering that U_0 essentially represents the binding energy and that interparticle bonds have to break up upon melting, provides a first simple argument in favor of this proportionality. Within the Lindemann melting scenario, a material becomes liquid when the vibration amplitude of the particles exceeds a certain limit. It is clear that for smaller U_0 , i.e. a more shallow potential well, such a limiting vibration amplitude is reached already at lower temperature, compared to a potential with larger U_0 (cf. Fig. 1b of the main paper). Thus, within the Lindemann scenario it is plausible that $T_m \propto U_0$. On the other hand, it has been shown by MacDonald and Roy⁶ that the thermal expansion is inversely proportional to the potential depth, $1/\alpha_c \propto U_0$, which can be explained by the fact that the attractive part of the pair potential becomes more shallow on decreasing U_0 as schematically visualized in Fig. 1b. This latter result was derived for different realistic interatomic potentials.⁶ Hence, overall we then have $T_m \propto U_0$ and $1/\alpha_c \propto U_0$, leading to $\alpha_c T_m = \text{const.}$ Indeed, as outlined above, it has been documented by Grüneisen⁴ that the Lindemann criterion (melting appears when the vibrational amplitude exceeds a critical ratio) and the relation $\alpha_c T_m = \text{const.}$, both follow from a generalized equation of state of the solid assuming a realistic anharmonic pair potential.

Experimentally, the latter relation has been checked for a number of material classes and the visualization of this relation has entered numerous textbooks and lecture notes. In literature, Straumanis⁷ was the first to plot thermal expansivity vs. the melting temperature (however using degree Celsius) of cubic elements and noted the continuous decrease of thermal expansion vs. increasing melting temperatures. Shortly after, this curve was fitted by van der Reyden⁸, however, again not using an absolute temperature scale. Finally it was documented by Bonfiglioli and Montalenti⁹ that the melting points of metals scale with the inverse thermal expansion, as theoretically derived. As documented in the main text of the work, this relation later on was checked and analyzed in detail for various materials classes, e.g., by Van Uiter¹⁰ and Granato *et al.*¹¹

For completeness of this small introduction into the field of melting phenomena, it is important to notice the work of Born,¹² who proposed that a "rigidity catastrophe" caused by a vanishing elastic shear modulus determines the melting of crystalline solids. It has been shown by Jin *et al.*¹³ that the melting of crystals probably is triggered by the Born and Lindemann criterion simultaneously.

Supplementary Note 2: Extraction of thermal-expansion data from literature

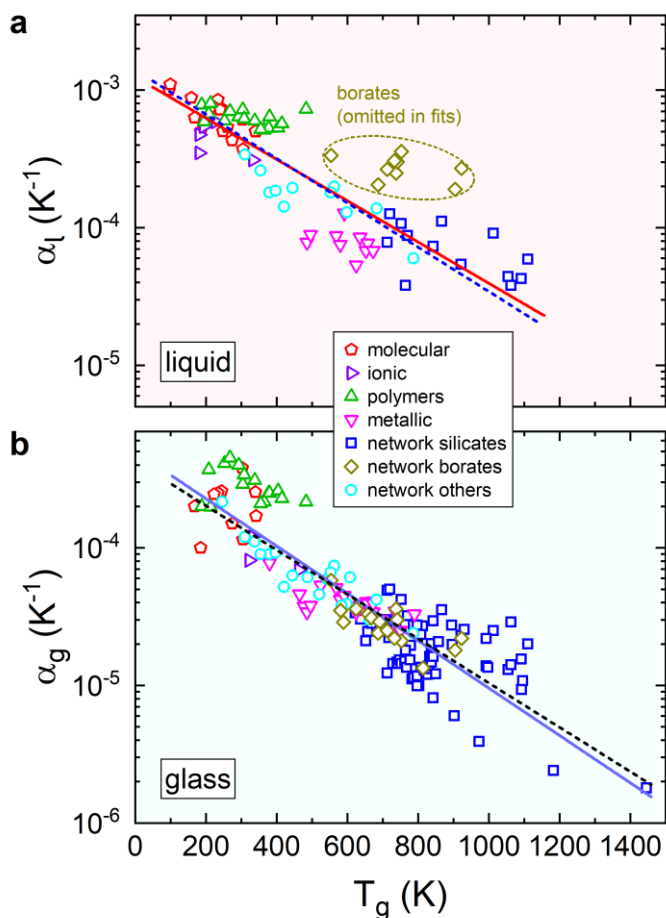
The main emphasis of this work is the detailed analysis of the available and published experimental data basis of the temperature-dependent volume expansion coefficient α for a large variety of disordered materials, measured in the high-temperature supercooled liquid phase ($T > T_g$) as well as in the low-temperature glass state ($T < T_g$). The data basis on thermal expansivity and glass transition temperature, which has been analyzed in the course of this work and which is presented in Figs. 1d, e and 2 of the main text, is documented in Supplementary Table 1. A few facts are worth being mentioned here. For many disordered materials the published data basis is significantly broader than listed in Supplementary Table 1 and in many cases we had to select between different sources as will be discussed below (Supplementary Note 3). In first respect and whenever possible, we tried to provide reference to the original literature, avoiding numerous inaccuracies and mistakes that have been made during the past decades: Supplementary Table 1 always indicates the volume thermal expansion as defined in Eq. 3 of the main text; it is the temperature derivative of the volume normalized to the volume. In cases where the linear thermal expansion was measured in the original literature, we simply multiplied this number by a factor of 3, taking into account the isotropic character of liquids and glasses. As is clearly documented in Supplementary Table 1 and also can be seen in Fig. 1d and e of the main text, the published data basis is much broader for the thermal expansion in the glass state than in the supercooled-liquid phase, partly due to experimental problems of the high glass-transition temperatures in some silicate-derived network glass formers and also because often only solid-state dilatometry was used. The sometimes large scatter of published data, as documented in Fig. 1d and e, partly certainly is due to the application of different techniques with varying precision used to determine the thermal expansion. In addition, in determining the volume expansion coefficient below and above T_g , the temperature dependence of the volume has to be linearized and, of course, the deduced slope, used to calculate the thermal expansion, depends on the width of the temperature window investigated and on the distance or closeness to T_g . The temperature regime for linearization varies considerably in range and width in the different experiments reported. Whenever possible, we took the two thermal expansion coefficients and the glass transition temperature from the same reference. Certainly there exist many more experimental values of thermal expansion in literature. Specifically concerning the network glasses, many experiments reported on systematic investigations of glasses with various components as function of concentration. In these cases, we have chosen the most relevant data and in many cases used the compounds with the highest and lowest T_g only, in order not to overburden the figures shown in the main part of the text.

Supplementary Note 3: Choice of α and T_g in case of multiple sources

In many cases, for a given material different values for the thermal expansion and the glass-transition temperature were reported and it is not straightforward to decide on the most reliable values. These variations result from different experimental techniques applied and/or differences in the samples investigated, e.g., different sample purity. Moreover, in polymers the chain length may vary considerably with considerable influence on thermal expansivity. In a number of molecular glasses, like alcohols or van-der-Waals glasses with low glass-transition temperatures, the water content may play a significant role and not always was specified in the published work. Concerning the glass-transition temperature, in addition different cooling rates and measuring and analyzing methods can also lead to considerable variations.

As an example, Supplementary Table 2 shows the various experimental reports on glass transition temperature and thermal expansivity for the molecular glass glycerol and for the chalcogenides network-glass selenium. Astonishingly, despite the fact that various techniques and various samples with mostly non-specified impurities were used, the scatter is within reasonable limits. An exception is the thermal-expansion coefficient of glycerol in the solid state, where the data from different sources deviate by more than a factor of three. In all cases, we decided not to take average values but to use the results with a clear description of the experimental measuring procedure, which are best documented, and from our point of view are most reliable.

Supplementary Figure 1 (with discussion)



Supplementary Figure 1 | Correlation of the thermal expansion with the glass-transition temperature. Semilogarithmic plot of the thermal volume-expansion coefficients α_g in the glass phase (a) and of α_l in the liquid phase (b) versus the glass-transition temperature T_g (same data sets as in Figs. 1d and e). The solid lines show linear fits based on all data points for each phase, except for α_l of the borates. The dashed lines represent linear fits presuming the same slope for α_l and α_g . Note that the ordinates of (a) and (b) were adjusted to achieve the same decades/cm ratio, enabling a direct comparison of the slopes.

Supplementary Fig. 1 shows the complete thermal-expansion data sets for the liquid (a) and glass state (b) using a semi-logarithmic representation, $\log_{10} \alpha$ vs. T_g . The experimental values are the same as those shown in the double-logarithmic plots of Figs. 1d and e and as listed in Supplementary Table 1. The observed approximately linear decrease directly demonstrates the roughly exponential dependence of α on T_g as also indicated by the dashed lines in Figs. 1d and e. The solid

lines in Supplementary Fig. 1 represent linear fits, $\log_{10} \alpha_i = b_i - s_i T_g$ (with $i = g$ or l for glass or liquid, respectively), neglecting α_l of the borates, which represent a special case (see main text). A simple visual comparison of frames (a) and (b) already reveals quite similar slopes s for the liquid and glass data sets. Indeed, the free fits (solid lines) lead to slopes of comparable order, $s_g = 1.72 \times 10^{-3} \text{ K}^{-1}$ and $s_l = 1.50 \times 10^{-3} \text{ K}^{-1}$, and both data sets can be almost equally well fitted using the same slope of $1.61 \times 10^{-3} \text{ K}^{-1}$ as shown by the dashed lines (the latter fit curves are also shown by the dashed lines in Figs. 1d and e). Therefore, the α - T_g correlations of the liquid and glass phases only differ by their axis intercepts: $b_l = -2.85$ and $b_g = -3.37$. Overall, we then have $\alpha_i = \alpha_{0,i} \exp(-n T_g)$, with $\alpha_{0,i} = 10^{b_i}$ and the same $n = s \ln 10$ for both data sets. Notably, if this exponential dependence would be an exact description of the experimental data, the values $\alpha_{0,l} \approx 1.4 \times 10^{-3} \text{ K}^{-1}$ and $\alpha_{0,g} \approx 4.3 \times 10^{-4} \text{ K}^{-1}$ would represent upper limits of the thermal expansion, which are approached for small T_g values. The inverse of n corresponds to a general energy scale of $\theta \approx 270 \text{ K}$, or about 23 meV, describing the thermal expansion of both glasses and liquids, which universally obey $\alpha_i = \alpha_{0,i} \exp(-T_g / \theta)$. As mentioned in the main text, the finding of the same θ (or n) for the liquid and glass states implies a universal ratio $\alpha_l/\alpha_g \approx 3$ for all glass formers.

Supplementary Table 1

Supplementary Table 1 | Glass temperature T_g , thermal volume expansion coefficient in the liquid (α_l) and the glass state (α_g), ratio α_l/α_g , and fragility index m for various materials belonging to different classes of glass formers. Only for part of the listed materials both expansion coefficients are available.

GLASS FORMER	T_g (K)	$10^4 \alpha_l$ (K ⁻¹)	$10^4 \alpha_g$ (K ⁻¹)	α_l/α_g	m
molecular (alcohols)					
sorbitol	274 [14]	4.3 [15]	1.5 [15]	2.9	93 [14]
xylitol	248 [16]	5.02 [17]			86 [16]
glycerol	185 [16]	5.0 [18]	1.0 [18]	5.0	53 [14]
propylene glycol	168 [16]	6.3 [19]	2.0 [19]	3.2	52 [14]
1-propanol	96 [20]	10 [21]			40 [14]
ethanol	99 [16]	11 [22]			52 [16]
molecular (v.d. Waals)					
$\alpha\alpha\beta$ -tris-naphthylbenzene	342 [23]	5.0 [23]	1.7 [23]	2.9	66 [14]
1,1'-di(4-methoxy-5-methylphenyl)cyclohexane (BMMPC)	261 [24]	5.4 [25]			72 [14]
ortho-terphenyl	245 [26]	7.34 [26]	2.58 [26]	2.8	81 [14]
1,1'-bis(p-methoxyphenyl)cyclohexane (BMPC)	240 [24]	7.2 [25]			96 [14]
67mol% ortho-terphenyl - 33mol% ortho-phenylphenol	234 [27]	8.5 [27]	2.5 [27]	3.4	
propylene carbonate	159 [16]	8.8 [28]			104 [14]
molecular (various)					
sucrose	340 [29]	5.02 [29]	2.54 [29]	2.0	88 [30]
glucose	305 [31]	3.72 [31]	1.15 [31]	3.4	79 [32]
colophony	303 [33]	6.1 [33]	3.8 [33]	1.6	
α -phenyl-o-cresol	223 [34]	7.53 [34]	2.45 [34]	3.1	83 [14]
salol	218 [14]	7.36 [35]			73 [14]
polymer					
poly(2,6-dimethylphenylene oxide)	483 [36]	7.29 [36]	2.16 [36]	3.4	218 [37]
Polycarbonate	415 [36]	5.72 [36]	2.28 [36]	2.5	132 [14]
poly(ortho-methylstyrene)	404 [38]	5.31 [38]	2.6 [38]	2.0	
poly(cyclohexyl methacrylate)	380 [39]	6.4 [39]	2.5 [39]	2.6	
poly(methyl methacrylate)	378 [40]	5.3 [40]	2.5 [40]	2.1	145 [14]
polyvinyl chloride	355 [41]	5.2 [41]	2.1 [41]	2.5	191 [14]
Polystyrene	365 [38]	5.13 [38]	2.16 [38]	2.4	139 [14]
poly(ethyl methacrylate)	338 [40]	6.0 [40]	3.1 [40]	1.9	81 [42]
poly(n-propyl methacrylate)	308 [40]	6.2 [40]	3.4 [40]	1.8	63 [42]
polyvinyl acetate	304 [43]	7.2 [43]	2.9 [43]	2.5	95 [14]
poly(n-butyl methacrylate)	293 [40]	6.4 [40]	4.0 [40]	1.6	75 [44]
poly(n-hexyl methacrylate)	268 [40]	7.0 [40]	4.5 [40]	1.6	
poly(n-octyl methacrylate)	253 [40]	6.0 [40]	4.1 [40]	1.5	
Polyurethane	213 [45]	8.02 [45]	1.98 [45]	4.1	
poly(n-dodecyl methacrylate)	208 [40]	6.7 [40]	3.7 [40]	1.8	
polyisobutene	195 [46]	5.9 [46]			46 [14]
polybutadiene	188 [41]	7.8 [41]	2 [41]	3.9	85 [32]
ionic					
AgPO ₃	463 [47]		0.69 [48]		
[Ca(NO ₃) ₂] _{0.4} [KNO ₃] _{0.6} (CKN)	333 [49]	3.64 [50]	1.2 [51]	3.0	93 [14]
(AgI) _{0.67} (Ag ₂ MoO ₄) _{0.33}	323 [52]		0.81 [53]		
1-Butyl-3-methylimidazolium chloride (Bmim Cl)	228 [54]	5.9 [55]			97 [54]
1-Methyl-3-octylimidazolium hexafluorophosphate (Omim PF ₆)	194 [54]	5.42 [56]			78 [54]

1-Butyl-3-methylimidazolium tetrafluoroborat (Bmim BF ₄)	182 [54]	3.5 [57]			93 [54]
1-Butyl-3-methylimidazolium tetrachloroferrate (Bmim FeCl ₄)	182 [54]	4.74 [58]			144 [54]
metallic					
Co ₄₃ Fe ₂₀ Ta _{5.5} B _{31.5}	790 [59]		0.33 [59]		
Fe ₇₅ P ₁₆ Si ₆ Al ₃	750 [10]		0.25 [60]		
Fe ₆₅ Co ₁₀ Ga ₅ P ₁₂ C ₄ B ₄	735 [59]		0.345 [59]		
N ₇₅ P ₁₆ B ₆ Al ₃	695 [10]		0.30 [60]		
Co ₅₉ Ni ₁₀ Fe ₅ Si ₁₁ B ₁₅	673 [61]	0.68 [61]	0.34 [61]	2.0	
Cu ₆₀ Hf ₂₅ Ti ₁₅	673 [59]		0.408 [59]		
Cu ₆₀ Zr ₃₀ Ti ₁₀	673 [59]		0.393 [59]		
Zr ₁₁ Cu ₄₇ Ti ₃₄ Ni ₈	658 [62]	0.77 [63]			47 [62]
Pd ₇₆ Au ₆ Si ₁₈	658 [59]		0.393 [59]		
Ti _{41.5} Zr _{2.5} Cu _{42.5} Ni _{7.5} Hf ₅ Si	654 [59]		0.405 [59]		
Zr ₅₅ Al ₁₀ Ni ₅ Cu ₃₀	653 [59]		0.339 [59]		
Zr ₆₅ Cu _{17.5} Al _{7.5} Ni ₁₀	653 [59]	0.68 [63]	0.339 [59]	2.0	
Pd _{77.5} Cu ₆ Si _{16.5}	636 [60]	0.85 [60]	0.38 [60]	2.2	60 [64]
Zr _{41.2} Ti _{13.8} Ni ₁₀ Cu _{12.5} Be _{22.5}	625 [65]	0.532 [65]	0.339 [65]	1.6	39 [64]
Pd ₁₆ Ni ₆₄ P ₂₀	591 [66]	1.27 [66]	0.24 [66]	2.8	
Pd ₄₈ Ni ₃₂ P ₂₀	580 [66]	0.75 [66]	0.42 [66]	1.8	
Pd ₄₀ Ni ₄₀ P ₂₀	569 [67]	0.87 [67]	0.51 [67]	1.7	50 [64]
Pd _{42.5} Ni _{7.5} Cu ₃₀ P ₂₀	525 [59]		0.534 [59]		
Pt ₄₅ Ni ₃₀ P ₂₅	496 [66]	0.89 [66]	0.38 [66]	2.3	
Pt _{52.5} Ni _{22.5} P ₂₅	486 [66]	0.78 [66]	0.34 [66]	2.3	
Pt ₆₀ Ni ₁₅ P ₂₅	478 [59]		0.375 [59]		
La ₅₅ Al ₂₅ Ni ₂₀	465 [59]		0.459 [59]		37 [64]
Mg ₆₅ Cu ₂₅ Y ₁₀	380 [59]		0.774 [59]		45 [62]
network silicates					
SiO ₂	1446 [68]		0.018 [69]		20 [14]
96.6SiO ₂ :2.9B ₂ O ₃ :0.4Al ₂ O ₃ :0.02Na ₂ O:0.02K ₂ O wt% (Corning Vycor®)	1183 [70]		0.024 [70]		
51.1SiO ₂ :25.2Al ₂ O ₃ :23.8CaO mol% (anorthite)	1111 [71]	0.59 [71]	0.2 [71]	3.0	54 [72]
55.6SiO ₂ :22.2Al ₂ O ₃ :22.2MgO mol% (cordierite, melted)	1096 [73]		0.108 [73]		
55.6SiO ₂ :22.2Al ₂ O ₃ :22.2MgO mol% (cordierite, sol-gel)	1093 [73]		0.093 [73]		
53.4SiO ₂ :23.1Al ₂ O ₃ :19.1CaO:4.5Na ₂ O mol%	1092 [74]	0.426 [74]	0.155 [74]	2.7	
60SiO ₂ :20Al ₂ O ₃ :20Na ₂ O mol%	1063 [75]	0.38 [75]	0.29 [75]	1.4	
Corning Jade® glass (alkaline earth aluminosilicate)	1055 [76]	0.44 [76]	0.13 [76]	3.4	32 [77]
49.8SiO ₂ :25.6CaO:24.6MgO mol% (diopside)	1013 [74]	0.91 [74]	0.25 [74]	3.6	53 [72]
69.0SiO ₂ :18.9Al ₂ O ₃ :12.3Na ₂ O wt% (albite)	922 [78]	0.54 [78]	0.23 [78]	2.1	22 [72]
65.8SiO ₂ :28.6K ₂ O:5.6Al ₂ O ₃ mol%	867 [74]	1.11 [74]	0.354 [74]	3.1	
60SiO ₂ :26.6Na ₂ O:13.3Al ₂ O ₃ mol%	843 [75]	0.73 [75]	0.29 [75]	1.4	
71.4SiO ₂ :14.3MgO:14.3Na ₂ O mol%	813 [79]		0.27 [79]		
82SiO ₂ :12B ₂ O ₃ :5Na ₂ O:1Al ₂ O ₃ mol% (Duran)	803 [80]		0.099 [80]		
68.4SiO ₂ :31.2PbO:0.4(Al ₂ O ₃ or Fe ₂ O ₃) mol%	779 [81]		0.2 [81]		
80SiO ₂ :20Na ₂ O mol%	770 [82]	0.876 [82]	0.32 [82]	2.7	37 [14]
90SiO ₂ :10Na ₂ O mol%	765 [82]	0.38 [82]	0.18 [82]	2.1	
70SiO ₂ :30Na ₂ O mol%	753 [82]	1.07 [82]	0.42 [82]	2.5	34 [72]
59.8SiO ₂ :39.9PbO:0.3(Al ₂ O ₃ or Fe ₂ O ₃) mol%	733 [81]		0.23 [81]		
60SiO ₂ :40Na ₂ O mol%	720 [82]	1.26 [82]	0.50 [82]	2.5	33 [72]
66.7SiO ₂ :33.3Na ₂ O mol% (Na ₂ Si ₂ O ₅)	713 [68]	0.78 [83]	0.49 [83]	1.6	45 [14]
71.4SiO ₂ :14.3CuO:14.3Na ₂ O mol%	694 [79]		0.27 [79]		
49.8SiO ₂ :49.8PbO:0.4(Al ₂ O ₃ or Fe ₂ O ₃) mol%	693 [81]		0.27 [81]		
39.4SiO ₂ :60.0PbO:0.6(Al ₂ O ₃ or Fe ₂ O ₃) mol%	623 [81]		0.34 [81]		
network silicates (Schott technical glasses from ref. [84])					
Schott 8240 (alkaline earth aluminosilicate glass)	1063 [84]		0.141 [84]		
Schott 8241 (alkaline earth aluminosilicate glass)	1063 [84]		0.141 [84]		
Schott NEO 1730 (alkaline earth, Nd containing, aluminosilicate glass)	998 [84]		0.135 [84]		
Schott 8252 (alkaline earth aluminosilicate glass)	993 [84]		0.138 [84]		
G018-346 (alkali-free sealing glass)	993 [84]		0.219 [84]		
Schott 8228 (sealing glass)	973 [84]		0.039 [84]		
G018-358 (alkali-free sealing glass)	931 [84]		0.255 [84]		
Schott 8229 (sealing glass)	903 [84]		0.06 [84]		
Schott 8436 (alkali alkaline earth silicate)	897 [84]		0.198 [84]		
Schott G018-311 (alkali-free sealing glass)	895 [84]		0.273 [84]		
Schott G018-266 (sealing glass)	858 [84]		0.207 [84]		
Schott 8341 (Pyran® S, borosilicate floatglass)	850 [84]		0.121 [84]		
Schott 8450 (sealing glass)	843 [84]		0.162 [84]		
Schott 8230 (sealing glass)	843 [84]		0.081 [84]		
Schott 8455 (sealing glass)	838 [84]		0.201 [84]		
Schott 8326 (neutral glass)	838 [84]		0.198 [84]		
Schott 8412 (Fiolax® clear, borosilicate glass)	838 [84]		0.147 [84]		
Schott 8800 (neutral glass)	838 [84]		0.165 [84]		
Schott 8454 (sealing glass)	838 [84]		0.192 [84]		
Schott 8414 (Fiolax® amber, borosilicate glass)	833 [84]		0.162 [84]		
Schott G018-200 (Zn-B-Si passivation and solder glass)	830 [84]		0.138 [84]		
Schott G018-197 (Zn-B-Si passivation glass)	830 [84]		0.132 [84]		
Schott 8660 (borosilicate glass)	828 [84]		0.12 [84]		

Schott 8651 (sealing glass)	822 [84]		0.132 [84]		
Schott 8488 (Suprax®, borosilicate glass)	818 [84]		0.129 [84]		
Schott 8449 (sealing glass)	808 [84]		0.135 [84]		
Schott 8415 (Illax®, soda-lime glass)	808 [84]		0.234 [84]		
Schott 8350 (AR-Glas®, soda-lime glass)	798 [84]		0.273 [84]		
Schott 8330 (Duran®, Borofloat® 33, Supremax®, borosilicate glass)	798 [84]		0.099 [84]		
Schott 8347 (borosilicate glass)	798 [84]		0.099 [84]		
Schott 8487 (borosilicate glass)	798 [84]		0.117 [84]		
Schott 8689 (borosilicate glass)	788 [84]		0.114 [84]		
Schott 8625 (VivoTag®, biocompatible glass)	787 [84]		0.275 [84]		
Schott 8448 (sealing glass)	783 [84]		0.111 [84]		
Schott 8245 (borosilicate glass)	778 [84]		0.153 [84]		
Schott 8652 (sealing glass)	768 [84]		0.135 [84]		
Schott 8250 (borosilicate glass)	763 [84]		0.15 [84]		
Schott 8270 (borosilicate glass)	763 [84]		0.15 [84]		
Schott 8447 (sealing glass)	753 [84]		0.144 [84]		
Schott 8650 (alkali-free sealing glass)	748 [84]		0.153 [84]		
Schott 8242 (borosilicate glass)	743 [84]		0.144 [84]		
Schott G017-725 (lead-borosilicate glass)	741 [84]		0.147 [84]		
Schott 8360 (soft glass, lead-free)	738 [84]		0.273 [84]		
Schott 8100 (lead glass, 33.5 % PbO)	738 [84]		0.288 [84]		
Schott 8405 (sodium-potassium-barium-silicate glass)	733 [84]		0.291 [84]		
Schott G017-096R (lead-borosilicate glass)	729 [84]		0.144 [84]		
Schott 8516 (sealing glass, high iron content)	720 [84]		0.267 [84]		
Schott 8456 (sealing glass)	718 [84]		0.222 [84]		
Schott 8337B (borosilicate glass)	713 [84]		0.123 [84]		
Schott 8470 (lead-free borosilicate glass)	713 [84]		0.30 [84]		
Schott 8531 (soft glass, sodium-free, high lead content)	708 [84]		0.273 [84]		
Schott 8532 (soft glass, sodium-free, high lead content)	708 [84]		0.261 [84]		
Schott 8095 (alkali-lead silicate, 28 % PbO)	703 [84]		0.273 [84]		
Schott G018-255 (lead-free Bi-Zn-B glass)	669 [84]		0.282 [84]		
Schott 8465 (lead-alumino-borosilicate glass)	658 [84]		0.246 [84]		
Schott G018-250 (lead-free solder glass)	653 [84]		0.21 [84]		
Schott G018-249 (lead-free solder glass)	638 [84]		0.303 [84]		
network borates					
60B ₂ O ₃ :40CaO mol%	923 [85]	2.7 [85]	0.22 [85]	12	
75B ₂ O ₃ :25CaO mol%	905 [85]	1.9 [85]	0.18 [85]	11	
Schott G018-205 (zinc-borate glass)	814 [84]		0.134 [84]		
73B ₂ O ₃ :27PbO mol%	753 [86]	3.58 [86]	0.21 [86]	17	
60B ₂ O ₃ :40Li ₂ O mol%	741 [87]	3.0 [87]	0.30 [87]	10	
66.7B ₂ O ₃ :33.3Na ₂ O mol%	738 [87]	2.5 [87]	0.36 [87]	6.9	
66.7B ₂ O ₃ :33.3PbO mol%	733 [86]	3.06 [86]	0.22 [86]	14	
58B ₂ O ₃ :42PbO mol%	713 [86]	2.65 [86]	0.25 [86]	11	
50B ₂ O ₃ :25PbO:10Na ₂ O:15Fe ₂ O mol%	691 [88]		0.29 [88]		
85B ₂ O ₃ :15Li ₂ O mol%	687 [89]	2.05 [89]	0.24 [89]	8.5	
50B ₂ O ₃ :25PbO:15Na ₂ O:10Fe ₂ O mol%	668 [88]		0.31 [88]		
50B ₂ O ₃ :25PbO:20Na ₂ O:5Fe ₂ O mol%	659 [88]		0.33 [88]		
50B ₂ O ₃ :25PbO:25Na ₂ O mol%	625 [88]		0.36 [88]		
Schott G018-256 (lead-borate glass)	589 [84]		0.288 [84]		
Schott G017-052 (lead-borate glass)	581 [84]		0.351 [84]		
B ₂ O ₃	554 [14]	3.35 [90]	0.58 [90]	5.8	32 [14]
network phosphates					
50P ₂ O ₅ :50BaO mol%	683 [86]	1.38 [86]	0.42 [86]	3.4	
45P ₂ O ₅ :45K ₂ O: 10MgSO ₄ mol%	608 [91]		0.61 [91]		
50P ₂ O ₅ :50Na ₂ O mol%	563 [86]	1.98 [86]	0.74 [86]	2.7	
50P ₂ O ₅ :40Na ₂ O:10BaO mol%	553 [86]	1.8 [86]	0.66 [86]	2.7	
network chalcogenides					
GeO ₂	787 [92]	0.6 [92]	0.24 [92]	2.5	20 [14]
50B ₂ O ₃ :33.3TeO ₂ :16.7PbO mol%	678 [93]		0.31 [93]		
60Se:40Ge mol%	598 [94]	1.29 [94]	0.39 [94]	3.3	
60Se:35Ge:5Sb mol%	584 [95]		0.38 [95]		
83.3TeO ₂ :10Li ₂ O:6.7PbO mol%	543 [93]		0.59 [93]		
60Se:20Ge:20Sb mol%	521 [95]		0.46 [95]		
70Se:20Ge:10Sb mol%	488 [95]		0.61 [95]		
60Se:40As mol%	445 [96]	1.95 [96]	0.63 [96]	3.1	36 [42]
60As:40Se mol%	421 [96]	1.42 [96]	0.52 [96]	2.7	
80Se:10Ge:10Sb mol%	397 [94]	1.86 [94]	0.92 [94]	2.0 [94]	
80Se:20As mol%	355 [96]	2.6 [96]	0.9 [96]	2.9	
Se	310 [97]	3.4 [96]	1.2 [96]	2.8	87 [14]
S	246 [10]		2.16 [10]		86 [98]
network halogenides					
BeF ₂	663 [10]		0.3 [10]		24 [42]
ZnCl ₂	380 [10]	1.8 [99]	0.9 [10]	2.0	30 [14]
60BeF ₂ :40KF mol%	338 [10]		1.11 [10]		

Supplementary Table 2

Supplementary Table 2 | Glass temperature T_g , thermal volume expansion coefficient in the liquid (α_l) and the glass state (α_g), and the ratio α_l/α_g for glycerol and selenium taken from a variety of different sources as indicated in the table. The bold numbers are those given in Supplementary Table 1 and shown in the figures of the main text.

GLASS FORMER	T_g (K)	$10^4\alpha_l$ (K ⁻¹)	$10^4\alpha_g$ (K ⁻¹)	α_l/α_g
glycerol	185 [16]	5.0 [18]	1.0 [18]	5.0
	~ 184 [18]			
		~ 4.5 [100]	~ 0.85 [100]	5.3
		5.0 [101]	1.0 [101]	5.0
	183 [102]	5.0 [102]	0.9 [102]	5.6
	185 [103]	5.4 [103]	3.3 [103]	1.6
	180 [104]	4.8 [104]	2.4 [104]	2.0
	180 - 190 [29]	4.83 [29]	2.4 [29]	2.0
Se	310 [97]	3.4 [96]	1.2 [96]	2.8
			1.4 [105]	
	304 [102]	4.0 [102]	1.3 [102]	3.1
	302 [103]	4.6 [103]	1.7 [103]	2.7
	303 [33]	4.46 [33]	1.74 [33]	2.6
	323 [94]	3.54 [94]	1.32 [94]	2.7
	300 [104]	4.2 [104]	1.7 [104]	2.5
	323 [96]			
	308 [106]			
	304 [107]			

References

1. F. A. Lindemann, *Über die Berechnung molekularer Eigenfrequenzen*, Phys. Z. **9**, 609 (1910).
2. J. J. Gilvarry, *The Lindemann and the Grüneisen laws*, Phys. Rev. **102**, 308 (1956).
3. F. H. Stillinger and T. A. Weber, *Lindemann melting criterion and the Gaussian core model*, Phys. Rev. B **22**, 3790 (1980).
4. E. Grüneisen, *Theorie des festen Zustandes einatomiger Elemente*, Annalen der Physik **39**, 257 (1912).
5. J. S. Dugdale and D. K. C. MacDonald, *The thermal expansion of solids*, Phys. Rev. **89**, 831 (1953).
6. D. K. C. MacDonald and S. K. Roy, *Vibrational anharmonicity and lattice thermal properties, II*, Phys. Rev. **97**, 673 (1955).
7. M. E. Straumanis, *The thermal expansion coefficient and the melting point of cubic elements*, J. Appl. Phys. **21**, 936 (1950).
8. D. van der Reyden, *The thermal expansion coefficient and the melting point of cubic elements*, J. Appl. Phys. **22**, 363 (1951).
9. G. Bonfiglioli and G. Montalenti, *On linear expansion coefficient and melting point of metals*, J. Appl. Phys. **22**, 1089 (1951).
10. L. G. Van Uitert, *Relation between melting point, glass transition temperature, and thermal expansion for inorganic crystals and glasses*, J. Appl. Phys. **50**, 8052 (1979).
11. A. V. Granato, D. M. Joncich, and V. A. Khonik, *Melting, thermal expansion, and the Lindemann rule for elemental substances*, Appl. Phys. Lett. **97**, 171911 (2010).
12. M. Born, *Thermodynamics of crystals and melting*, J. Chem. Phys. **7**, 591 (1939).
13. Z. H. Jin, P. Gumbsch, K. Lu, and E. Ma, *Melting Mechanisms at the Limit of Superheating*, Phys. Rev. Lett. **87**, 055703 (2001).
14. R. Böhmer, K. L. Ngai, C. A. Angell, and D. J. Plazek, *Nonexponential relaxations in strong and fragile glass formers*, J. Chem. Phys. **99**, 4201 (1993).
15. M. Naoki, K. Ujita, and S. Kashima, *Pressure-volume-temperature relations and configurational energy of liquid, crystal, and glasses of D-sorbitol*, J. Phys. Chem. **97**, 12356 (1993).
16. P. Lunkenheimer, S. Kastner, M. Köhler, and A. Loidl, *Temperature development of glassy α -relaxation dynamics determined by broadband dielectric spectroscopy*, Phys. Rev. E **81**, 051504 (2010).
17. S. Höhle, A. König-Haagen, and D. Brüggemann, *Thermophysical characterization of MgCl₂·6H₂O, xylitol and erythritol as phase change materials (PCM) for latent heat thermal energy storage (LHTES)*, Materials **10**, 444 (2017).
18. A. K. Schulz, *Über die Kunststoffe als unterkühlte Flüssigkeiten*, Kolloid Zeitschrift **138**, 75 (1954).
19. G. S. Parks and H. M. Huffman, *Studies on Glass I. The transition between the glassy and liquid states in the case of some simple organic compounds*, J. Phys. Chem. **31**, 1842 (1927).
20. S. Takahara, O. Yamamuro, and H. Suga, *Heat capacities and glass transitions of 1-propanol and 3-methylpentane under pressure. New evidence for the entropy theory*, J. Non-Cryst. Solids **171**, 259 (1994).
21. J. Peleteiro, D. Gonzalez-Salgado, C. A. Cerdeirina, and L. Romani, *Isobaric heat capacities, densities, isentropic compressibilities and second-order excess derivatives for (1-propanol + n-decane)*, J. Chem. Thermodynamics **34**, 485 (2002).
22. M. Hashemi, M. Moosavi, A. Omrani, and A. A. Rostami, *Non-ideal behavior of ethanol + amines mixtures, modeling using the Peng-Robinson and PC-SAFT equation of state*, J. Mol. Liq. **256**, 445 (2018).
23. D. J. Plazek and J. H. Magill, *Physical properties of aromatic hydrocarbons. I. Viscous and viscoelastic behavior of 1:3:5-tri- α -naphthyl benzene*, J. Chem. Phys. **45**, 3038 (1966).
24. G. Meier, B. Gerharz, D. Boese, and E. W. Fischer, *Dynamical processes in organic glassforming van der Waals liquids*, J. Chem. Phys. **94**, 3050 (1991).
25. M. Paluch, C. M. Roland, R. Casalini, G. Meier, and A. Patkowski, *The relative contributions of temperature and volume to structural relaxation of van der Waals molecular liquids*, J. Chem. Phys. **118**, 4578 (2003).

26. M. Naoki and S. Koeda, *Pressure-volume-temperature relations of liquid, crystal, and glass of o-terphenyl. excess amorphous entropies and factors determining molecular mobility*, J. Phys. Chem. **93**, 948 (1989).
27. S. Takahara, M. Ishikawa, O. Yamamuro, and T. Matsuo, *Structural relaxations of glassy polystyrene and o-terphenyl studied by simultaneous measurement of enthalpy and volume under high pressure*, J. Phys. Chem. B **103**, 792 (1999).
28. W. Song, H. Zhang, Z. Yang, J. Wang, Z. Yue, and Ji Yu, *Intermolecular interaction for binary mixtures of propylene carbonate with acetonitrile, dimethyl carbonate, diethyl carbonate at different temperatures: Density and viscosity*, Z. Phys. Chem. **232**, 127 (2018).
29. W. Kauzmann, *The nature of the glassy state and the behavior of liquids at low temperatures*, Chem. Rev. **43**, 219 (1948).
30. I. Dranca, S. Bhattacharya, S. Vyazovkin, and R. Suryanarayanan, *Implications of global and local mobility in amorphous sucrose and trehalose as determined by differential scanning calorimetry*, Pharm. Res. **26**, 1064 (2009).
31. G. S. Parks, H. M. Huffman, and F. R. Cattoir, *Studies on glass. II. The transition between the glassy and liquid states in the case of glucose*, J. Phys. Chem. **32**, 1366 (1928).
32. E. Rössler, K.-U. Hess, and V. N. Novikov, *Universal representation of viscosity in glass forming liquids*, J. Non-Cryst. Solids **223**, 207 (1998).
33. G. Tammann and A. Kohlhaas, *Die Begrenzung des Erweichungsintervalles der Gläser und die abnorme Änderung der spezifischen Wärme und des Volumens im Erweichungsgebiet*, Z. Anorg. Allg. Chem. **182**, 49 (1929).
34. W. T. Laughlin and D. R. Uhlmann, *Viscous flow in simple organic liquids*, J. Phys. Chem. **76**, 2317 (1972).
35. L. Comez, S. Corezzi, D. Fioretto, H. Kriegs, A. Best, and W. Steffen, *Slow dynamics of salol: A pressure- and temperature-dependent light scattering study*, Phys. Rev. E **70**, 011504 (2004).
36. K. Hagiwara, T. Ougizawa, T. Inoue, K. Hirata, and Y. Kobayashi, *Studies on the free volume and the volume expansion behavior of amorphous polymers*, Rad. Phys. Chem. **58**, 525 (2000).
37. E. C. Glor, R. C. Composto, and Z. Fakhraei, *Glass transition dynamics and fragility of ultrathin miscible polymer blend films*, Macromolecules **48**, 6682 (2015).
38. A. Quach and R. Simha, *Pressure-volume-temperature properties and transitions of amorphous polymers; Polystyrene and poly (orthomethylstyrene)*, J. Appl. Phys. **42**, 4592 (1971).
39. R. A. Orwoll, *Densities, coefficients of thermal expansion, and compressibilities*, in *Physical properties of polymers handbook*, edited by J. E. Mark (Springer, New York, 2007), p. 93.
40. S. S. Rogers and L. Mandelkern, *Glass formation in polymers. I. The glass transitions of the poly-(n-alkyl methacrylates)*, J. Phys. Chem. **61**, 985 (1957).
41. L. A. Wood, *Glass transition temperatures of copolymers*, J. Polymer Sci. **28**, 319 (1958).
42. D. Huang and G. B. McKenna, *New insights into the fragility dilemma in liquids*, J. Chem. Phys. **114**, 5621 (2001).
43. J. E. McKinney and M. Goldstein, *PVT Relationships for liquid and glassy poly(vinyl acetate)*, J. Res. Natl. Bur. Stand. Sect. A **78**, 331 (1974).
44. K. Schröter, S. Reissig, E. Hempel, and M. Beiner, *From small molecules to polymers: Relaxation behavior of n-butyl methacrylate based systems*, J. Non-Cryst. Solids **353**, 3976 (2007).
45. R. Simha and R. F. Boyer, *On a general relation involving the glass temperature and coefficients of expansion of polymers*, J. Chem. Phys. **37**, 1003 (1962).
46. J. D. Ferry and G. S. Parks, *Studies on Glass XIII. Glass formation by a hydrocarbon polymer*, J. Chem. Phys. **4**, 70 (1936).
47. J. Liu, J. Portier, B. Tanguy, J.-J. Videau, and C. A. Angell, *Glass formation and conductivity in the Ag₂S-AgPO₃ system: Evidence against cluster pathway mechanisms for high ionic conductivity*, Solid State Ionics **34**, 87 (1987).
48. R. Bogue and R. J. Sladek, *Elasticity and thermal expansivity of (AgI)_x(AgPO₃)_{1-x} glasses*, Phys. Rev. B **42**, 5280 (1990).
49. A. Pimenov, P. Lunkenheimer, M. Nicklas, R. Böhmer, A. Loidl, and C. A. Angell, *Ionic transport and heat capacity of glass-forming metal-nitrate mixtures*, J. Non-Cryst. Solids **220**, 93 (1997).
50. P. K. Gupta and C. T. Moynihan, *Prigogine-Defay ratio for systems with more than one order parameter*, J. Chem. Phys. **65**, 4136 (1976).
51. K. J. Rao, D. B. Hephrey, and C. A. Angell, *Thermodynamic properties of M(I) M(II) mixed nitrate glasses and supercooled liquids*, Phys. Chem. Glasses **14**, 26 (1973).
52. P. Mustarelli, C. Tomasi, E. Quartarone, A. Magistris, M. Cutroni, and A. Mandanici, *Structure and cation dynamics in the system AgI:Ag₂MoO₄: a ¹⁰⁹Ag NMR study*, Phys. Rev. B **58**, 9054 (1998).
53. A. Raimondo, A. Mandanici, M. A. Ramos, J. G. Rodrigo, C. Armellini, M. Cutroni, and S. Vieira, *Experimental study of the thermal expansion of (AgI)_{0.67}(Ag₂MoO₄)_{0.33} ionic glass from 5 K to 300 K*, Phil. Mag. **88**, 3973 (2008).
54. P. Sippel, P. Lunkenheimer, S. Krohns, E. Thoms, and A. Loidl, *Importance of liquid fragility for energy applications of ionic liquids*, Sci. Rep. **5**, 13922 (2015).
55. H. Machida, R. Taguchi, Y. Sato, and R. L. Smith, Jr., *Measurement and correlation of high pressure densities of ionic liquids, 1-ethyl-3-methylimidazolium L-lactate ([emim][lactate]), 2-hydroxyethyl-trimethylammonium L-lactate [(C₂H₄OH)(CH₃)₃N][Lactate]], and 1-butyl-3-methylimidazolium chloride ([bmim]-[Cl])*, J. Chem. Eng. Data **56**, 923 (2011).
56. A. Saini, A. Harshvardhan, and R. Dey, *Thermophysical, excess and transport properties of organic solvents with imidazolium based ionic liquids*, Indian J. Chem. **57A**, 21 (2017).
57. M. Wang, N. Rao, M. Wang, Q. Cheng, S. Zhang, and J. Li, *Properties of ionic liquid mixtures of [NH₂e-mim][BF₄] and [bmim][BF₄] as absorbents for CO₂ capture*, Greenhouse Gas Sci Technol. **8**, 483 (2018).
58. Q. G. Zhang, J. Z. Yang, X.-M. Lua, J.-S. Guic, and M. Huang, *Studies on an ionic liquid based on FeCl₃ and its properties*, Fluid Phase Equilib. **226**, 207 (2004).
59. H. Kato, H.-S. Chen, and A. Inoue, *Relationship between thermal expansion coefficient and glass transition temperature in metallic glasses*, Scr. Mater. **58**, 1106 (2008).
60. H. S. Chen, *The influence of structural relaxation on the density and Young's modulus of metallic glasses*, J. Appl. Phys. **49**, 3289 (1978).
61. N. O. Gonchukova and A. N. Drugov, *Thermal expansion of amorphous alloys*, Glass Phys. Chem. **29**, 184 (2003).
62. I. Gallino, *On the fragility of bulk metallic glass forming liquids*, Entropy **19**, 483 (2017).
63. B. Damaschke and K. Samwer, *Thermal expansion measurements of glass-forming alloys in the melt and the undercooled state under microgravity conditions*, Appl. Phys. Lett. **75**, 2220 (1999).
64. J. Krausser, K. H. Samwer, and A. Zaccone, *Interatomic repulsion softness directly controls the fragility of supercooled metallic melts*, PNAS **112**, 13762 (2015).

65. K. Ohsaka, S. K. Chung, W. K. Rhim, A. Peker, D. Scruggs, and W. L. Johnson, *Specific volumes of the $Zr_{41.2}Ti_{13.8}Cu_{12.5}Ni_{10.0}Be_{22.5}$ alloy in the liquid, glass, and crystalline states*, Appl. Phys. Lett. **70**, 726 (1997).
66. H. S. Chen, J. T. Krause, and E. A. Sigety, *Thermal expansion and density of glassy Pd-Ni-P and Pt-Ni-P alloys*, J. Non-Cryst. Solids **13**, 321 (1974).
67. G. Wilde, S. G. Klose, W. Soellner, G. P. Görler, K. Jeropoulos, R. Willnecker, and H. J. Fecht, *On the stability limits of the undercooled liquid state of Pd-Ni-P*, Mater. Sci. Eng. A **226-228**, 434 (1997).
68. C. A. Angell, *Strong and fragile liquids*, in *Relaxations in complex systems*, edited by K. L. Ngai and G. B. Wright (NRL, Washington, DC, 1985), p. 3.
69. J. Otto and W. Thomas, *Die thermische Ausdehnung von Quarzglas im Temperaturbereich von 0 bis 1060 °C*, Zeitschrift für Physik **175**, 337 (1963).
70. H. Scholze, *Glas. Natur, Struktur und Eigenschaften* (Springer, Berlin, 1988).
71. M. J. Toplis and P. Richet, *Equilibrium density and expansivity of silicate melts in the glass transition range*, Contrib. Mineral Petrol **139**, 672 (2000).
72. S. Webb and R. Knoche, *The glass-transition, structural relaxation and shear viscosity silicate melts*, Chemical Geology **128**, 165 (1996).
73. M. Nogami, S. Ogawa, and N. Nagasaka, *Preparation of cordierite glass by the sol-gel process*, J. Mat. Sci. **24**, 4339 (1989).
74. R. A. Lange, *A revised model for the density and thermal expansivity of $K_2O-Na_2O-CaO-MgO-Al_2O_3-SiO_2$ liquids from 700 to 1900 K: extension to crustal magmatic temperatures*, Contrib. Mineral Petrol **130**, 1 (1997).
75. W. D. Drotning, *Density and thermal expansion measurements of several mixed oxide glasses in the solid and liquid regions*, Sandia Report, SAND 84-2006, Sandia Nat. Labs. (1984) (<https://doi.org/10.2172/5994693>).
76. M. Potuzak, J. C. Mauro, T. J. Kiczanski, A. J. Ellison, and D. C. Allan, *Communication: Resolving the vibrational and configurational contributions to thermal expansion in isobaric glass-forming systems*, J. Chem. Phys. **133**, 091102 (2010).
77. C. J. Wilkinson, K. Doss, O. Gulbitten, D. C. Allan, and J. C. Mauro, *Fragility and temperature dependence of stretched exponential relaxation in glass-forming systems*, J. Am. Ceram. Soc. **104**, 4559 (2021).
78. R. Knoche, D. B. Dingwell, and S. L. Webb, *Non-linear temperature dependence of liquid volumes in the system albite-anorthite-diopside*, Contrib. Mineral Petrol **111**, 61 (1992).
79. M. D. Karkhanavara and F. A. Hummel, *Thermal expansion of some simple glasses*, J. Am. Ceram. Soc. **35**, 215 (1952).
80. D. Ehrhart, *Structure, properties and applications of borate glasses*, Glass Technol. **41**, 182 (2000).
81. G. J. Bair, II, *The correlation of physical properties with atomic arrangement*, J. Am. Ceram. Soc. **19**, 347 (1936).
82. R. Knoche, D. B. Dingwell, F. A. Seifert, and S. L. Webb, *Non-linear properties of supercooled liquids in the system Na_2O-SiO_2* , Chemical Geology **116**, 1 (1994).
83. L. Shartsis, S. Spinner, and W. Capps, *Density, expansivity, and viscosity of molten alkali silicates*, J. Am. Ceram. Soc. **35**, 155 (1952).
84. *Technical Glasses. Physical and technical properties* (Schott AG, Mainz, 2014).
85. V. P. Klyuev and B. Z. Pevzner, *Thermal expansion and glass transition temperature of calcium borate and calcium aluminoborate glasses*, Glass Phys. Chem. **29**, 127 (2003).
86. W. D. Drotning, *Thermal expansion of glasses in the solid and liquid phases*, Int. J. Thermophysics **6**, 705 (1985).
87. V. P. Klyuev and B. Z. Pevzner, *The influence of aluminum oxide on the thermal expansion, glass transition temperature, and viscosity of lithium and sodium aluminoborate glasses*, Glass Phys. Chem. **28**, 207 (2002).
88. S. Ibrahim, M. M. Gomaa, and H. Darwish, *Influence of Fe_2O_3 on the physical, structural and electrical properties of sodium lead borate glasses*, J. Adv. Ceram. **3**, 155 (2014).
89. Yu. K. Startsev and O. Yu. Golubeva, *Specific features of changes in the properties of one- and two-alkali borate glasses containing water: III. Thermal expansion and the structural and mechanical relaxation parameters of two-alkali borate glasses*, Glass Phys. Chem. **28**, 232 (2002).
90. A. Napolitano, P. B. Macedo, and E. G. Hawkins, *Viscosity and density of boron trioxide*, J. Am. Ceram. Soc. **48**, 613 (1965).
91. V. G. Vyatchina, L. A. Perelyaeva, M. G. Zuev, and I. V. Baklanova, *Structure and properties of glasses in the $MgSO_4-Na_2B_4O_7-KPO_3$ system*, Glass Phys. Chem. **35**, 580 (2009).
92. J. E. Shelby, *Properties and structure of $B_2O_3-GeO_2$ glasses*, J. Appl. Phys. **45**, 5272 (1974).
93. J. E. Stanworth, *Tellurite glasses*, Nature **169**, 582 (1952).
94. U. Senapati and A. K. Varshneya, *Configurational arrangements in chalcogenide glasses: a new perspective on Phillips' constraint theory*, J. Non. Cryst. Solids **185**, 289 (1995).
95. J. A. Savage, P. J. Webber, and A. M. Pitt, *An assessment of Ge-Sb-Se glasses as 8 to 12 μm infra-red optical materials*, J. Mater. Sci. **13**, 859 (1978).
96. A. E. Voronova, V. A. Ananichev, and L. N. Blinov, *Thermal expansion of melts and glasses in the As-Se system*, Glass Phys. Chem. **27**, 267 (2001).
97. R. Böhmer and C. A. Angell, *Elastic and viscoelastic properties of amorphous selenium and identification of the phase transition between ring and chain structures*, Phys. Rev. B **48**, 5857 (1993).
98. B. Ruta, G. Monaco, V. M. Giordano, F. Scarponi, D. Fioretto, G. Ruocco, K. S. Andrikopoulos, and S. N. Yannopoulos, *Nonergodicity factor, fragility, and elastic properties of polymeric glassy sulfur*, J. Phys. Chem. B **115**, 14052 (2011).
99. Y. Umetsu and T. Ejima, *Phase diagram of the $PbCl_2-ZnCl_2$ binary system and density of the binary melt*, Trans. JIM **15**, 276 (1974).
100. I. V. Blazhnov, N. P. Malomuzh, and S. V. Lishchuk, *Temperature dependence of density, thermal expansion coefficient and shear viscosity of supercooled glycerol as a reflection of its structure*, J. Chem. Phys. **121**, 6435 (2004).
101. K. Trachenko and V. V. Brazhkin, *Heat capacity at the glass transition*, Phys. Rev. B **83**, 014201 (2011).
102. K. G. Sturm, *Thermische Ausdehnung und Glasübergang als Bestimmungsgrößen der Viskosität von Flüssigkeiten*, Rheol. Acta **20**, 59 (1981).
103. S. C. Sharma, L. Mandelkern, and F. C. Stehling, *Relations between expansion coefficients and glass temperature*, Polymer Lett. **10**, 345 (1972).
104. R. O. Davies and G. O. Jones, *Thermodynamic and kinetic properties of glasses*, Adv. Phys. **2**, 370 (1948).
105. E. J. Felty and M. B. Myers, *Thermal expansion of arsenic-selenium glasses*, J. Am. Ceram. Soc. **50**, 335 (1967).
106. C. T. Moynihan and U. E. Schnaus, *Heat capacity and equilibrium polymerization of vitreous Se*, J. Amer. Ceramic Soc. **54**, 136 (1971).
107. A. Eisenberg and A. V. Tobolsky, *Viscoelastic properties of amorphous selenium*, J. Polymer. Sci. **61**, 483 (1962).